International Journal of Energy and Environmental Science
2023; 8(2): 31-43
http://www.sciencepublishinggroup.com/j/ijees
doi: 10.11648/j.ijees.20230802.11
ISSN: 2578-9538 (Print); ISSN: 2578-9546 (Online)

Automatic Generation Control of Simplified Egyptian Power System Using Fractional Order PI Controller Based on PSO

Ali Mohamed Ali[1, *], Mohamed Shawky Saad[2], Adel El Amari[3], Mohamed Ahamed Moustafa Hassan[2]

[1]Cairo North Power Station, Ministry of Electricity and Energy, Cairo, Egypt

[2]Department of Electrical Power Engineering, Faculty of Engineering, Cairo University, Cairo, Egypt

[3]Ministry of Electricity and Energy, Cairo, Egypt

Email address:

eng.ali_mohammed@hotmail.com (Ali Mohamed Ali)

[*]Corresponding author

To cite this article:

Ali Mohamed Ali, Mohamed Shawky Saad, Adel El Amari, Mohamed Ahamed Moustafa Hassan. Automatic Generation Control of Simplified Egyptian Power System Using Fractional Order PI Controller Based on PSO. *International Journal of Energy and Environmental Science*. Vol. 8, No. 2, 2023, pp. 31-43. doi: 10.11648/j.ijees.20230802.11

Received: October 26, 2022; **Accepted**: December 26, 2022; **Published**: April 27, 2023

Abstract: In this Paper, Fraction Order (FO) PI controller is tested in order to find the optimized gains for Automatic Generation Control (AGC) controller by Particle Swarm Optimization (PSO) algorithm to represent the Simplified Egyptian Power System (SEPS) to achieve the development of power grid for the sustainable growth of Egypt. The mission of AGC is to return primary frequency regulation capability, bring back the frequency to its predefined set point in addition to reduce power fluctuation due to unplanned tie-line power flows among nearby control zones. The suggested controller is built using actual statistical records of SEPS for minimum and maximum loading situations of the SEPS in Winter and Summer of 2019-2020. The strength of the proposed controller is illustrated by implement the suggested controller and verify the outcomes of trip of the biggest generation unit in this Simplified Egyptian Power System (SEPS) on the grid frequency. The gains of fractional order FO-PI controller parameters such as proportional, integral, order of integrator (λ) are elevated by different Particle Swarm Optimization (PSO) and compared with another conventional supplementary Proportional Integral (PI) based on PSO also. The results display that the suggested FO-PI controller-built on PSO provides finest dynamic performance for a step load variation. The used software for gaining the results is MATLAB-Simulink.

Keywords: Automatic Generation Control (AGC), Fractional Order PI Controller, Particle Swarm Optimization (PSO), Simplified Egyptian Power System (SEPS), Load Frequency Control (LFC)

1. Introduction

Keeping the predefined produced megawatt of power plants in addition to assisting in controlling the frequency of the control zone is the main task of automatic Load Frequency Control (LFC). However, through the real process of the zone, there will be variances between forecasted and actual loads. Therefore, the task of LFC is to recompense the common load forecast difficulties. The typical structure method of a load-frequency controller uses the linear control theory to improve control rules on the basis of the linearized mathematical model. The controller design is usually based on Algebraic Riccati- Equation using state-feedback fixed-parameters controller as illustrated [1-2].

However, in the fact that the system parameters may be changed (or cannot be totally identified), the controller layout constructed on a static parameter model could not ensure the stability of the entire system if the real power station model differs from the suggested power station model. The system transient frequency variation cannot be competently adjusted. Likewise, the state feedback controller used depends on measuring signals from all the states which may be essentially difficult to achieve. The three major difficulties to implement load-frequency controller of power systems [3]:

a) Non-linearity in the interactions

b) Uncertainty in the parameters, and

c) *System parameter differences because of changes in Process conditions.*

The healthy load frequency controller design is studied in several methods [4]. The most popular technique to implement frequency control is primary frequency regulation (generator governor response) and LFC. The essential mission of LFC is to bring back primary frequency tuning capability, recovering again the frequency to its nominal set point and reducing unplanned tie-line energy flows between nearby control zones. From the approaches used to process the economics of this facility in other markets, competitive offers or common contracts be obvious [5]. The nominal speed will not reach the value as of the primary controller, and remaining offset. There is one technique to recover the frequency or speed to its predefined set point by modifying the integral controller. The integrator detects the mean error at a specific time so the offset will have vanished. This approach is achieved by Automatic Generation Control (AGC) or manually by Load Frequency Control (LFC) [6-7].

PSO is used to obtain a strong load frequency controller for SEPS. The suggested controller is obtained and considered on two dissimilar loading situations of the SEPS through the winter and summer of 2019-2020 [8]. Complete stability of the SEPS is achieved while the proposed controller is implemented to it for these four loading situations in the existence of all system constraint uncertainties and the GRC.

Alhelou et al. [9] provide a comprehensive survey on different challenges and viewpoints of AGC in both conventional and untraditional power stations and presents initially reviews the usage of AGC in the different configuration of the electric power system. Furthermore, the applications of various modern and intelligent control methods are reviewed. In-depth survey on dissimilar approaches for AGC systems by adding Battery Energy Storage Systems (BESSs) because of their high energy density regarding to BESS advantage is given [10]. These advantages are: fast response, ownership obligations, and cooperation with the national grid system. While Obaid et al. [11] many difficulties in the AGC of unconventional smart electric power systems are studied where various AGC approaches; integrating the BESS-based electrical vehicles (EVs); are considered.

Wu et al [12] described the difficulties and application of diverse AGC systems in wind energy generation plants and the fact of the poor primary performance and low inertial of wind turbines which affect on the AGC regulations. Furthermore, the study investigated variable speed wind turbines and appropriate frequency control methods which can improve the frequency response. Bevrani and Hiyama [13] concentrated on several intelligent AGC systems and their application in distributed and renewable power energy schemes.

Shankar et al.[14] illustrate a complete analysis on AGC relating its distribution generation systems, conventional power systems, and a various structure of the micro-grid system. Additionally, the study also exposed the application of various energy storage devices, High Voltage Direct Current (HVDC), Flexible AC Transmission Systems (FACTS) devices and connects in the AGC scheme. Though, the study still suffers weak in several contemporary regulation structures and optimization methods for AGC. It's observed that the same approach relating the analysis on AGC is followed which illustrated several difficulties related with adding of FACTS devices, fast energy storage systems, photovoltaic (PV) systems, and wind-diesel power plant into the AGC systems [15].

The article is arranged as following: In Part II presents the SEPS power system grid and illustrated the entire arrangement for power production stations of SEPS in 2019-2020. Moreover, Part III presents the used MATLAB simulation model which used in this article, Part IV explained the used control algorithms such as Fractional Order PI and several forms of particle swarm optimization while Part V illustrates the simulation outcomes and discussion. Finally, Part VI finalize the conclusion.

2. The SEPS Power System Grid Under Study

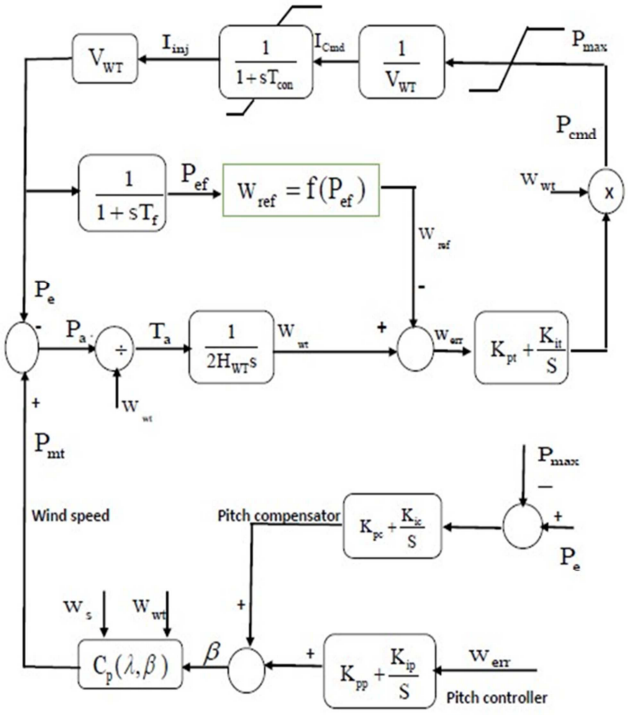

Figure 1. *DFIG scheme Block model.*

The entire mounted production capacity of SEPS in 2019 understudy was expanded to be 58353 MW as well as emergency and reserve power plants the total production approximately to 60000 MW [8, 31]. The Maximum peak daily load was 32000 MW in July while the Minimum daily load was 14595 MW in December 2019.

The Simplified EPS contains of 80 power station containing 413 generating units which are categorized into the following categories [8, 31]:

a) Combined cycle generation plants considered by the common in SEPS about 55.7% of the established capability.
b) Non-reheat generating unit (Gas turbine power stations) with a few steam generation plants (approximately 7% of the established capacity).
c) Reheat generation plants (Thermal generating units) are approximately 28.7% of the total capability.
d) Hydro-generation plants (around 4.8% of the total capacity).
e) Renewable generation plants (wind in addition to solar) denoted as 3.8% of established capability.

The SEPS dynamic power frequency model has built by the National Energy Control Center (NECC) of the related Electricity Authority [16]. The NECC model is mainly designed for solving the difficulties of load shedding as well as studied the impact of primary reserve. The model is reconstructed with some modification based on Matlab / Simulink. The original model is adjusted by minor loop control with a simple integral controller to allow the addition of a secondary controller [16].

The Simplified Egyptian Power System (SEPS) developed is enhanced by adding the DFIG model to signify the wind generation stations as displayed in 2017 report of EPS [17-18]. The SEPS model is achieved and presented in Matlab/Simulink® program. The block diagram of DFIG model is given in Figure 1 [19].

The SEPS composed of seven strongly linked areas [16], the interconnection specifics among the various zones were neglected and the proposal is accomplished relying on a single zone (area) power system scheme. The scheme has been tested via two various loading situation scenarios with outage or tripping of the biggest generation power unit (650 MW) in the SEPS [17].

3. Simulation Scheme for SEPS Power System

The LFC scheme of the SEPS block diagram in addition to the DFIG scheme without including the combined cycle and non-reheat turbines as presented by Matlab Simulink in Figure 2 [18]. Due to increasing of load change of EPS or tripping of power generation unit, the turbine speed will be dropped earlier the turbine governors make correction modification to regulate the steam input to new load value therefore it's important to implement of robust LFC controller with optimized gains.

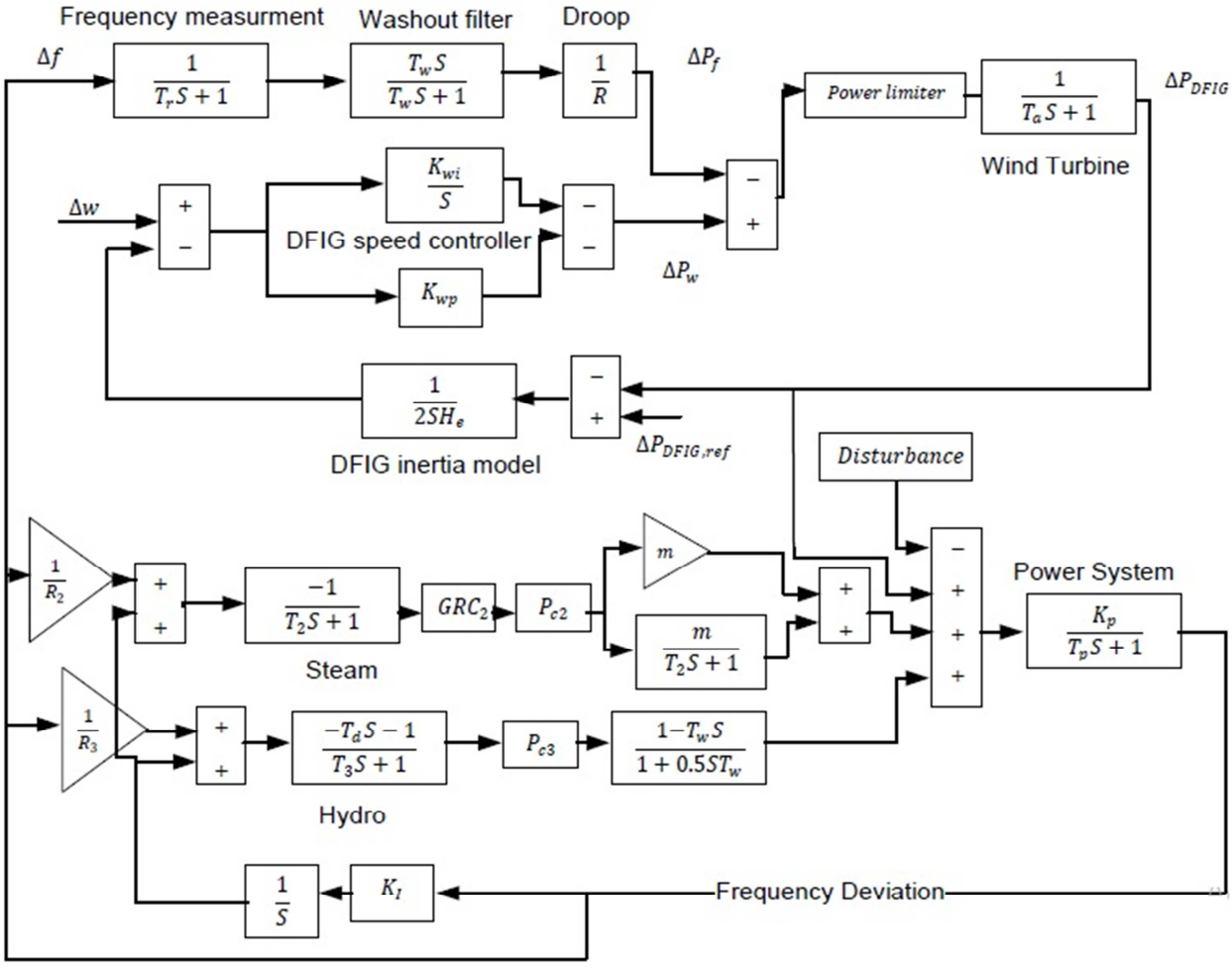

Figure 2. *Simplified EPS frequency control scheme containing DFIG wind scheme.*

4. Proposed Control Algorithms

The Proportional Integral controller enhance the performance of the closed loop system in addition to can dealing with nonlinearly systems with any changes in system parameter or in operating point through online upgrading the PI controller parameters [18].

a) Particle Swarm Optimization

Particle Swarm Optimization (PSO) is considered as one of stochastic Evolutionary Computation algorithms which depend on intelligence and motion of swarms. In contrast with GA which it the highest advantage of PSO algorithm, PSO doesn't have genetic processes like crossover and mutation. Particles velocity is interiorly updated by particles themselves and fast converge to the best (optimum) solution [20].

The major change among PSO and other ECs demonstrated in the methodology of particles can alter the population/swarm from the iteration to the next iteration in the search space through the iteration run, while in EA, the particles are altered in every iteration [21].

The coordinates of every particle in PSO display a promising result via two vectors, the velocity (v_i) and position (x_i) vectors.

In search space with N-dimension $X_i = [x_i^1, x_i^2, ..., x_i^N]$ and $V_i = [v_i^1, v_i^2, ..., v_i^N]$ with every particle i there are the two vectors associated.

A swarm contained of feasible solutions "or a number of particles" that fly (advance) over the possible solution space to discover optimal solutions. Every particle informs its location according to its hold best search; best swarm whole experience, and its earlier velocity vector based on the following model [22]. Equations (1) and (2) define the PSO.

$$V_i^{t+1} = w \times V_i^t + C_1 \times R_1 \times (Pbest_i^t - X_i^t + C_2 \times R_2 \times (Gbest^t - X_i^t) \quad (1)$$

$$X_i^{t+1} = X_i^t + V_i^{t+1} \quad (2)$$

Where:-

C_1 Cognitive Constant (≈2).

C_2 Social Constant (≈2).

C_1 and C_2 are two positive constants.

w is the inertia weight (0 to 1)

R_1 and R_2 are two randomly generated numbers with a range of {0,1}

$Pbest_i^t$ is the best position particle succeeded according to its own experience

$$Pbest_i^t = [x_{i1}^{pbest}, x_{i2}^{pbest}, ..., x_{iN}^{pbest}].$$

$Gbest^k$ is the best particle position relay on the entire swarm's experience.

$$gbest^t = [x_1^{gbest}, x_2^{gbest}, ..., x_2^{gbest}].$$

t is referring to the index of iteration.

the term of *gbest* characterized by social component while The term of *pbest* is characterized by cognitive component. Hence the values of C_1 and C_2 regulate the direction of every particles in both global and local components, the term of ($\omega \times v_i$) is earlier velocity [20].

The inertia weight w is beginning with large weight at starting of the searching then proportionally reduced when iteration progressed relating to Equation

$$w = w_{\max} - \frac{(w_{\max} - w_{\min})iter}{iter\_\max} \quad (3)$$

Where

$iter\_\max$ is maximum iteration number is maximum iteration number.

$w_{\max}$ is final weight, $w_{\min}$ is minimum weight.

This is termed Time Varying Inertia Weight (TVIW-PSO), but occasionally it suffers from local optimal which means swarm doesn't getting a solution [23].

The PSO flow chart is clarified in Figure 3, as presented in [20, 22, 25].

b) Constrictive Particle Swarm Optimization

The highest advantage of Constrictive Particle Swarm Optimization (C- PSO) is to enhance the convergence of PSO in primarily iterations of search and assists to escape from local optimal point then the convergence of PSO technique will enhanced [23]. By setting Constrictive factor (K) multiply by Equation (2) according to constrictive factor (K) Equation [24]:

$$K = \frac{2}{abs(2 - C - sqrt(C^2 - 4 * C))} \quad (4)$$

Where C = $C_1 + C_2$, C > 4 [24].

c) Adaptive Acceleration Coefficients Particle Swarm

Adaptive Acceleration Coefficients Particle Swarm (AAC-PSO) is known by the acceleration coefficients C_1 and C_2 are updated linearly with time that the cognitive.

Component is decreased whereas social component is increased as search iteration progress.

The AAC-PSO updates the acceleration coefficients exponentially with time based on their minimum and maximum values. The reason of using exponential function to decrease or increase speed of such function to accelerate the convergence procedure to get better search.

In exploration space. Also C_1 and C_2 are adaptively consistent with the fitness value of $Gbest$ and $Pbest$

[20, 22, 25, 26, 28].

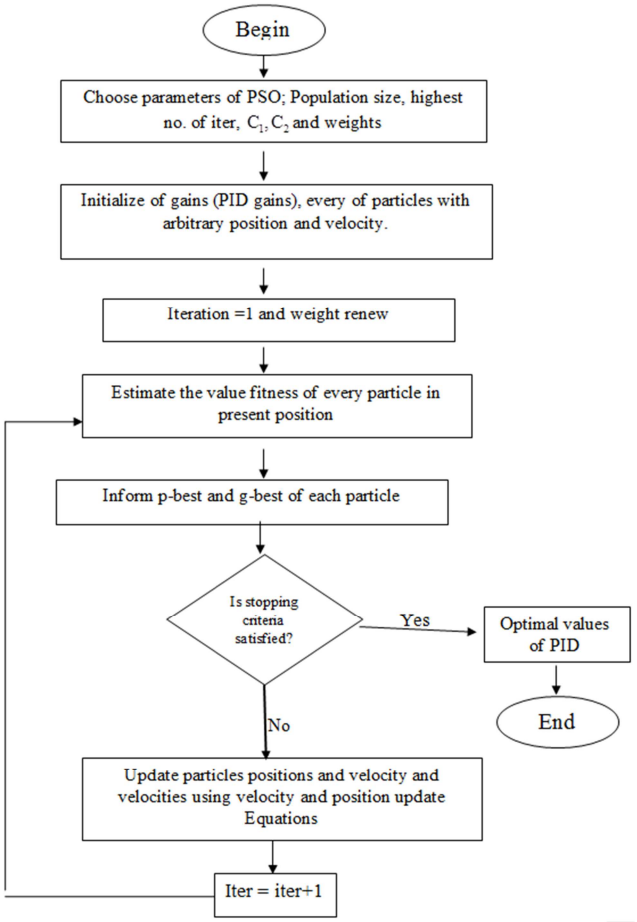

Figure 3. *Flow Chart of PSO Algorithm.*

$$V_i^{(t+1)} = w^{(t)}V_i^{(t)} + C_i^{(t)}r_1 \times (Pbest_i^{(t)} - X_i^{(t)}) + C_2^{(t)}r_2 \times (Gbest^{(t)} - X_t^{(t)}) \quad (5)$$

Where

$$w^{(t)} = w_o.\exp(-\alpha_w \times t) \quad (6)$$

$$C_1^{(t)} = c_{1o}.\exp(-\alpha_c \times t \times k_c^{(t)}) \quad (7)$$

$$C_2^{(t)} = c_{2o}.\exp(\alpha_c \times t \times k_c^{(t)}) \quad (8)$$

$$\alpha_c = -\frac{1}{t_{\max}}.\ln\left(\frac{c_{2o}}{c_{10}}\right) \quad (9)$$

$$k_c^{(t)} = \frac{(F_m^{(t)} - G_{best}{}^{(t)})}{F_m^{(t)}} \quad (10)$$

Where $c_i^{(t)}$ is acceleration coefficient at iteration t, with i=1 or 2. $w^{(t)}$ is inertia weight factor and t is iteration number. α_w is calculated with respect to initial and final values of w with the same way as α_c and *ln* is neperian logarithm. $k_c^{(t)}$ is determined according the fitness value of G_{best} and P_{best} at iteration *t*. c_{oi}, ω_O *are* acceleration coefficients and initial values of inertia weight factor respectively with i=1or 2. $F_m^{(t)}$ is the mean value of the best positions according to all particles at iteration t [27].

d) Modified Adaptive Acceleration Coefficients Particle Swarm

Modified Adaptive Acceleration Coefficients Particle Swarm (MAAC-PSO) Equation is the similar as (AAC) but it is modified to:

$$C_1 + C_2 = C_{TOTAL} \quad (11)$$

$$C_2 = C_{TOTAL} - C_1, \quad (12)$$

Where C_{Total} $(3.5 \rightarrow 6)$

C1 is given by Equation (7)

It's supposed to be fewer calculation for c_1 and c_2 then offered faster solutions than (AAC) [20, 22, 25, 28, 31].

Design of the gain Controller Based on Particle Swarm Optimization Techniques

The proposed controller gains will be implemented based on the set-a parameters (Nominal parameters). Assume a process which has the transfer function is GP(s). A measure of the robust stability of the closed loop system can be represented as:

$$M_s = \max_w \left| \frac{1}{1 + G_P(jw).G_C(jw)} \right| \quad (13)$$

Classical value for the maximum sensitivity Ms, is in the range of 1.4 to 2 [29]. Assume λi presents the real part of the poorly damped electromechnical mode eigenvalue of the system and identify the eigenvalue-based objective function as

$$J = min\{max\lambda_i\} \quad (14)$$

In this case study, it is intended to minimize the objective function (performance index J) as given in Equation (14) to increase the damping of the poorly damped electromechanical modes. The performance index J is minimized under the following constraints

$$1.4 \leq M_s \leq 2$$
$$K_{Pr\min} \leq K_{Pr} \leq K_{Pr\max}$$
$$K_{I\min} \leq K_I \leq K_{I\max}$$
$$K_{D\min} \leq K_D \leq K_{D\max}$$

Typical ranges of the optimized parameters are [-100, 100].

In this article, the controller gain is chosen between [0, 100]. It's clear that it is a nonlinear optimization problem. The input to the gain controller is the system frequency deviation and its output is the corrective control signal. It's cleared that the PSO using the multi- objective (Cost) function which PSO tries to minimize the Overshoot, Settling Time, Rise Time and the Error which in this case is frequency deviation (Δf)) as shown in following Fitness Function (FF) Equation (15):

$$FF = min[w_1 \times O.S + w_2 \times T_s + w_3 \times T_r + w_4 \times \Delta f] \quad (15)$$

where $w_1 = w_2 = w_3 = w_4 = 0.25$ [30].

5. Simulation Results and Discussion

Two different scenarios are considered based on the improved dynamic MATLAB-Simulink model of the National Energy Control Center (NECC) as illustrated in Figure 4, based on the Static and Operation Parameters of SEPS.

Frist scenario: tripping (outage) of the biggest power generation unit (Kuriemat 650 MW) at highest load of SEPS in July 2019 and monitoring the frequency response with Proportional integral controller.

Second scenario: tripping (outage) of the biggest power generation unit (Kuriemat 650 MW) at lowest load of SEPS in December 2019 and monitoring the frequency response with proportional integral controller.

These two scenarios are applied using Fractional Order Proportional Integral controller (FO-PI) based on PSO optimization techniques and compared with the performance of Proportional Integral (PI) controller based on PSO Techniques.

Four techniques of PSO are discussed and compared according to their performance in each scenario (Max or Min) loading conditions with both (FO-PI) and (PI) controllers.

The model parameters are divided into two groups. The first group of parameters is not depending on system operating conditions which are displayed in Table 1. These parameters values are evaluated by [16].

Table 1. *The Simplified Egyptian LFC Parameters.*

Parameter	Value	Parameter	Value	Parameter	Value
D	0.028	R1	2.5	Tw	1.0
T1	0.4	R2	2.5	R_I	0.8
T2	0.4	R3	1.0	T_I	2.5
T_h	6	T_d	5	Tr	15
M	0.5	T3	90	Tw	6
R_w	3	He	1.5	Ta	0.2
Kwi	0.1	Kwp	1.58		

The second group parameters are updated with time corresponding to the SEPS operating conditions. The desired data to define the changing parameters are involved with the data of each generator including: status (on or off), unit rating (MW), type of unit (Reheat, Non-Reheat, or Hydro); unit production (MW) for the operating condition under case study; inertia of the unit and the spinning reserve of the unit in percentage of the unit rating [8].

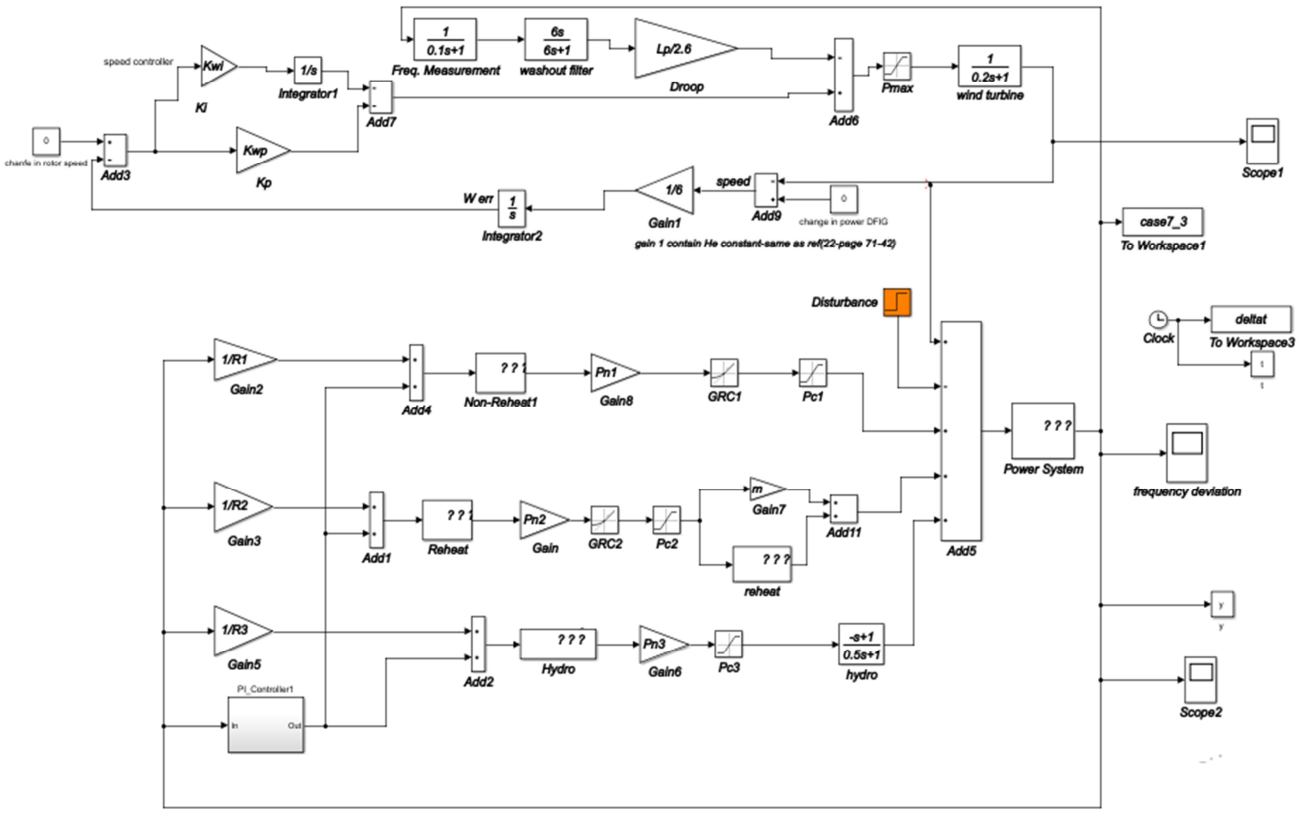

Figure 4. *MATLAB-Simulink scheme of the IPS- LFC including PI controller.*

The Simulink model take into consideration the difference between the Generating Rate Constraints (GRC) for various generating units. The simulated values for GRC are MW/min.1 pu and 0.2 pu 0 MW/min. for reheat turbines and non-reheat turbines, correspondingly. The GRC of hydro plants is disregarded as its actual value is much greater contrasted to the time periods of actual disturbances.

The Two SEPS loading conditions are simulated to design the PSO-based Controller gain. These two loading conditions stated the highest and lowest loads in two daily load curves of the SEPS in 2019-2020 [8].

Seven excel files are combined to calculate the changing parameters of the Simulink model. Every excel file contains the seven parameters values for each of the 304 generating units installed in 2019. The first parameter indicates the capacity (rating) of the unit, whereas the second parameter denotes the maximum operating MW. The third one shows maximum reserve power and the fourth for minimum operating MW of the unit. The fifth represents minimum reserve power of the unit and the sixth shows the unit inertia, while the seventh represents the unit's type [31].

Table 2 illustrates the calculated parameters produced from these seven files for the two operating conditions.

Table 2. *The SEPS Operating Conditions.*

	H	Pn1	Pn2	3	Pc1	Pc2	Pc3	Pmax	Lp	Δ PL
Max Load (Highest)	3.8142	0.259	0.1488	0.01	.611	0.291	0.648	0.018	0.001	0.0203
Min Load (Min)	3.593	0.044	0.19	0.039	0.611	0.291	0.648	0.018	0.002	0.0445

Where:

Lp: the penetration index of wind turbine in SEPS which is in this article states to minimum and maximum operating of wind turbine in each load condition.

Pn: Nominal Rated Power for each group of similar Power Stations.

Table 3 displays the Fractional PI and PI controller gains obtained by different PSO types in High (max) and Low (min) loading conditions.

PI Controller Case

In this case the PI controller is used for tuning the frequency deviation of SEPS in both loading scenarios.

Table 3. *Values of FOPI and PI gains.*

	Fraction PI				PI			
	High		Low		High		Low	
PSO	KP	2.309	KP	0.713	KP	1.3940	KP	0.12
	KI	0.899	KI	0.402	KI	1.2346	KI	0.09225
	VI	1.50	VI	0.7638				
PSOC	KP	2.85	KP	0.60369	KP	0.26841	KP	0.58261
	KI	1.263	KI	0.45107	KI	0.41514	KI	0.24347
	VI	1.4297	VI	0.88308				
AAPSO	KP	2.98	KP	0.51453	KP	2.95	KP	0.1501
	KI	1.387	KI	0.19499	KI	0.5048	KI	0.2354
	VI	1.479	VI	0.96289				
MAAPSO	KP	1.921	KP	0.8068	KP	0.0103	KP	1.631
	KI	0.7342	KI	0.5003	KI	0.1132	KI	0.235
	VI	1.392	VI	1				

High Loading Scenario

The results of simulation are presented in Table 4, It displays the dropping in the SEPS frequency response in terms of Minimum frequency values (Nadir values) and Rate Of Change of Frequency (ROCOF) till the tuned PI controller take the action to vanish the frequency deviation.

Table 4 illustrate performance evaluation for PI controller obtained by various types of PSO Techniques in case of High Loading Scenario (HLS).

Table 4. *Performance of PI controller tuned by various types of PSO in case of HLS.*

	High Loading Scenario			
	PSO	PSOC	AAPSO	MAAPSO
Nadir (Hz)	-0.03302	-0.05665	-0.02497	-0.08258
Time of Nadir (Sec)	5.830	6.5	5.630	7.460
Max O. S. (Hz)	0.02408	0.03177	0.005875	0.01413
ROCOF (Hz/Sec)	-0.04121	-0.0551	-0.0415	-0.05895
Settling Time (Sec)	10.05616	13.5454	0	12.22926

Figure 5 illustrates the comparisons between 4 gains (as displayed in Table 3) for Frequency Deviation in High Loading Scenario (HLS).

For facilitating calculation of ROCOF and Nadir point, a zoom in the curve is described in Figure 6.

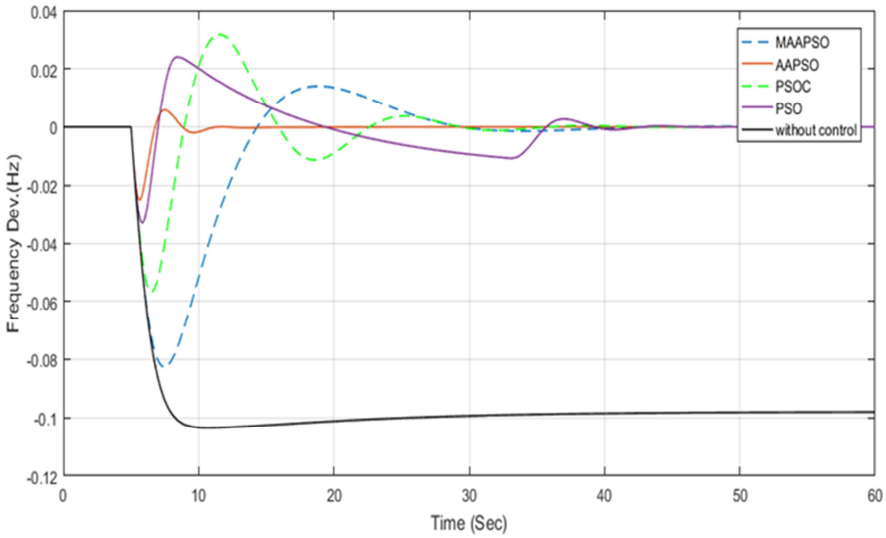

Figure 5. *Comparisons between 4 gains for Frequency Deviation in HLS.*

From Figure 5 and Table 4; It is noticeable that without control the system can't returned back to its nominal frequency value so the need of PI control is apparent. The MAAPSO gain offering acceptable maximum overshoot value (0.01413) but it also gives the highest (worst) Nadir point which it's not preferable it power system grid while the PSOC gain gives second highest Nadir point but also gives highest maximum overshoot compared with other gains.

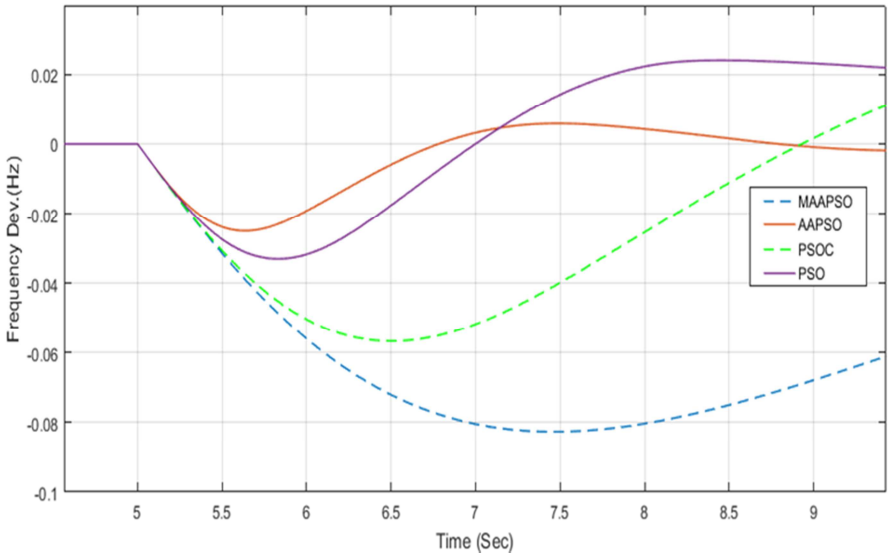

Figure 6. *Zoomed in System frequency response (ROCOF).*

Although the PSO gain presents the lowest (best) ROCOF but its performance regarding to other parameters don't gives the best performance at all.

The AAPSO gain shows the best obtained gain performance compared with other gains regarding to parameters like Nadir point, maximum overshoot and settling time.

It's clear that through run the iterations of every type of PSO separately, the best objective function index were gained are: PSOC, PSO, AAPSO respectively while the highest Objective function index was MAAPSO gain.

Although the PSOC gives best objective function index (also fast time to getting a solution) but shows highest settling time compared with other gains (according to ±2% of steady state of nominal frequency value); as given in Table 4.

It is obvious and interesting in Table 4, the value of ROCOF doesn't have substantial difference between the four obtained gains because it's presents the strength of the SEPS

grid in case of disturbance happened.

Low Loading Scenario

Table 5 illustrates the performance evaluation for the PI controller obtained by various types of PSO in case of optimized low loading condition.

Table 5. *Performance for PI controller obtained by various types of PSO in case of Low Loading Scenario (LLS).*

Low Loading Scenario				
	PSO	**PSOC**	**AAPSO**	**MAAPSO**
Nadir (Hz)	-0.1258	-0.08612	-0.1152	-0.05882
Time of Nadir (Sec)	6.510	5.960	6.3	5.63
Max O. S. (Hz)	0.000465	0.0162	0.04357	0.02126
ROCOF (Hz/Sec)	-0.14188	-0.13228	-0.1409	-0.11268
Settling Time (Sec)	11.50292	7.471605	14.06386	8.57178

Figure 7 clarifies the comparisons between 4 gains for Frequency Deviation in case of low loading scenario.

As apparent in Figure 7 that without controller gain, the frequency deviation (error) will be inherent because of the PI controller is not actuated in the system yet.

For clarifying the calculation of ROCOF and Nadir point in lowest loading scenario, a zoom for the curve is presented in Figure 8.

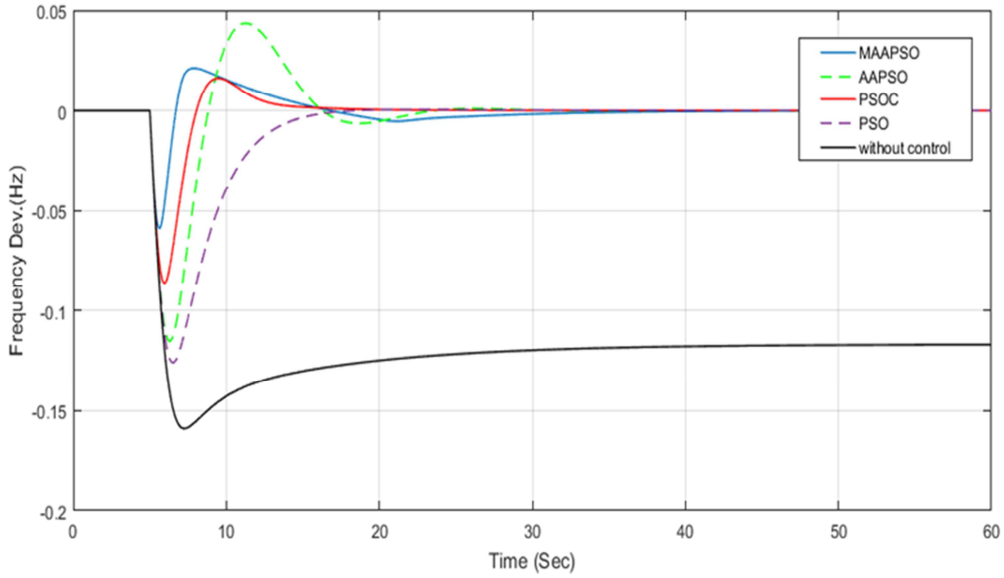

Figure 7. *Comparisons between 4 gains for Frequency Deviation in LLS.*

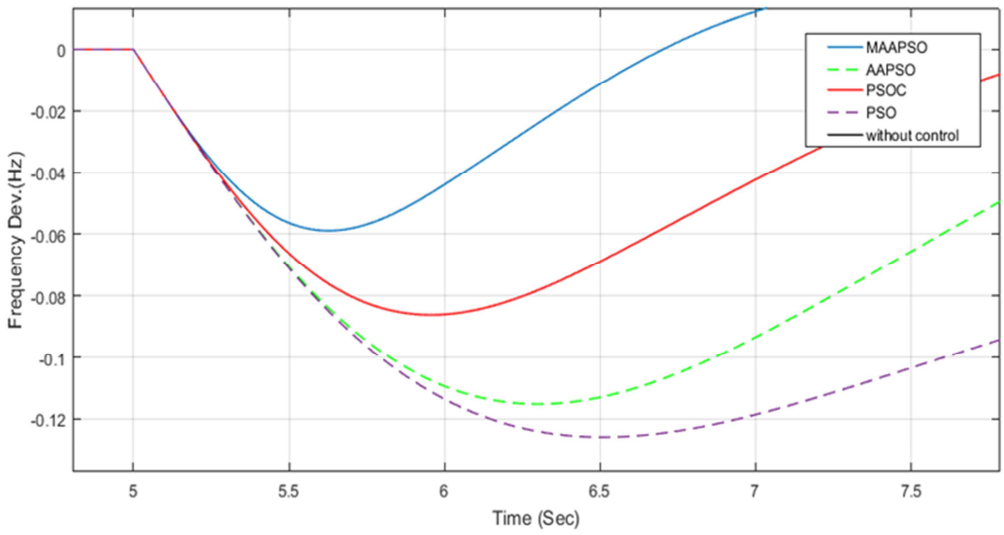

Figure 8. *Zoomed in System frequency response (ROCOF).*

As presented in Figure 7, 8 and the results in table 5, the power system frequency response suffering from inherent frequency deviation (error) when not controller in system so the frequency deviation can't return back to zero.

Although the PSO gain offers the lowest (best) maximum overshoot value compared with other obtained gains but it shows highest (worst) Nadir Point value and value which mean highly deterioration in frequency of SEPS also it take along settling time (11.502 Sec) until frequency deviation vanished.

The AAPSO gain presents the highest (worst) maximum overshoot value and longest (worst) settling time compared to the other gains even though it shows good performance related to Nadir point and ROCOF values. The PSOC gain indicates the lowest (best) settling time value and gives 2nd lowest values for both the maximum overshoot and ROCOF compared with other gains.

The MAAPSO gain denotes the lowest values (best) for both Nadir point and ROCOF and 2nd lowest value for settling time overall gains and displays good performance related to maximum overshoot value.

It is noticeable that during run the iterations of each type of PSO individually, the best objective function index were gained are: MAAPSO, AAPSO, PSOC, respectively whereas the highest Objective function index was gain PSO.

Fraction Order PI controller (FO-PI) Case

In this section, the FO-PI controller is used for tuning the frequency deviation of SEPS in both loading scenario and compared the performance with PI controller which illustrated last section.

As mentioned previously in table 3, the gain values of FO-PI and PI controllers which obtained by different PSO types were presented in both High (maximum) and Low (minimum) loading conditions.

High Loading Scenario

Table 6 illustrate the performance evaluation for FO-PO controller optimized by various types of PSO in case of HLS.

Figure 9 denote the comparisons between 4 gains for Frequency Deviation in high loading scenario in case of FO-PI controller.

For simplifying calculation of Nadir point and ROCOF, a zoom in for the curves is displayed in Figure 10.

Table 6. *Performance for FO-PI controller optimized by various types of PSO for HLS.*

High Loading Scenario (FO-PI)				
	PSO	**PSOC**	**AAPSO**	**MAAPSO**
Nadir (Hz)	-0.02814	-0.02535	-0.02483	-0.0291
Time of Nadir (Sec)	5.72	5.640	5.630	5.730
Max O. S. (Hz)	0.01353	0.01475	0.01541	0.02083
ROCOF (Hz/Sec)	-0.05084	-0.04816	-0.04754	-0.05204
Settling Time (Sec)	6.19904	5.976109	5.937918	8.76729

As presented in Figure 9 it is clear that the system without any controller can't resolve or handle with frequency deviation occurred by the disturbance load and error be inherent in the frequency system response. Although the PSO gain present the lowest (best) maximum overshoot value but it shows the 2nd highest values for other parameters like Nadir point, ROCOF and Settling time values respectively compared with other gains. PSOC gain displays good performance which it was 2nd lowest (best) Nadir point and ROCOF values overall gains.

MAAPSO gain display highest (worst) values for all parameters like Nadir, Maximum overshoot, ROCOF and Settling time which mean worst performance overall gains while AAPSO gain shows the lowest (best) values for all parameters and presents the best performance compared with other gains.

The best objective function index were gained during the run of iterations for each type of PSO individually are: PSO, AAPSO, PSOC, respectively while the highest Objective function index (which mean longer time to getting a solution) was gain MAAPSO.

Table 7. *Performance for FO-PI controllers in case of Low Loading Scenario.*

Low Loading Scenario (FO-PI)				
	PSO	**PSOC**	**AAPSO**	**MAAPSO**
Nadir (Hz)	-0.07774	-0.08192	-0.08998	-0.07534
Time of Nadir (Sec)	5.84	5.89	6.01	5.81
Max O. S. (Hz)	0.02567	0.03751	0.007541	0.04032
ROCOF (Hz/Sec)	-0.12872	-0.13104	-0.1337	-0.1273
Settling Time (Sec)	9.54804	11.79301	7.7929	13.91695

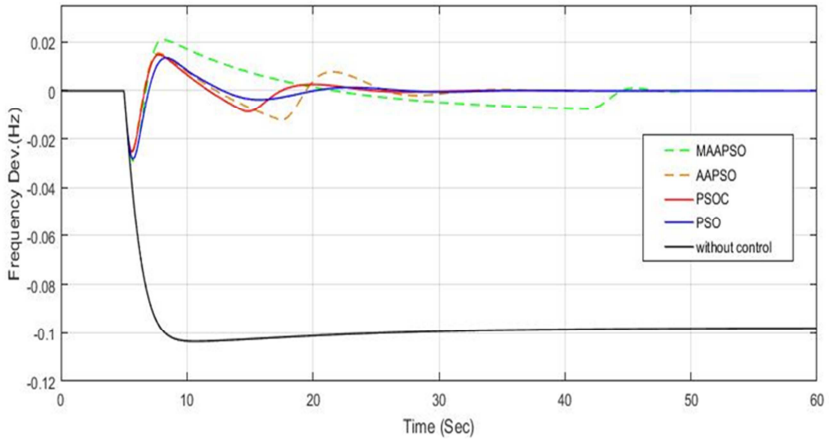

Figure 9. *Comparisons between 4 gains for Frequency Deviation in HLS in case of FO-PI controller.*

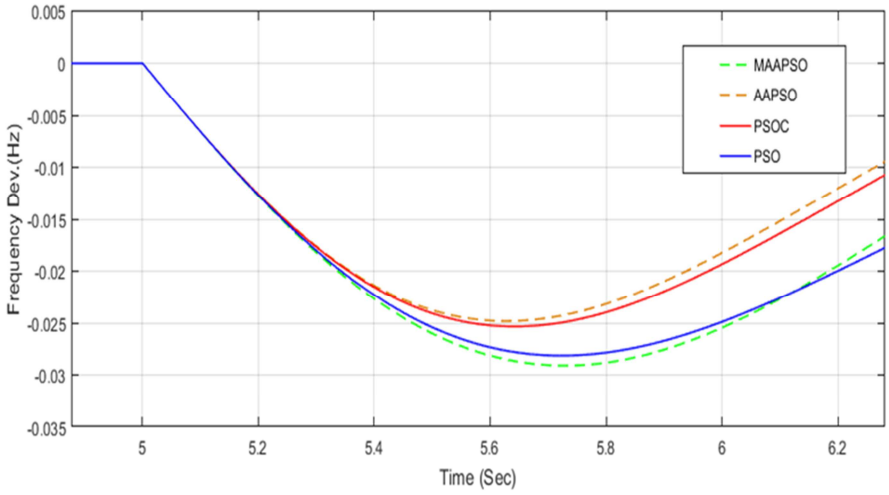

Figure 10. *Zoomed in System frequency response (ROCOF) in case of FO-PI controller.*

Low Loading Scenario

Table 7 clarifies performance evaluation for FO-PO controller gained through different types of PSO in case of low loading condition.

Figure 11 denoted the comparisons between 4 gains for Frequency Deviation in low loading scenario in case of FO-PI controller.

For simplifying calculation of Nadir point and ROCOF, a zoom for the curves is displayed in Figure 12.

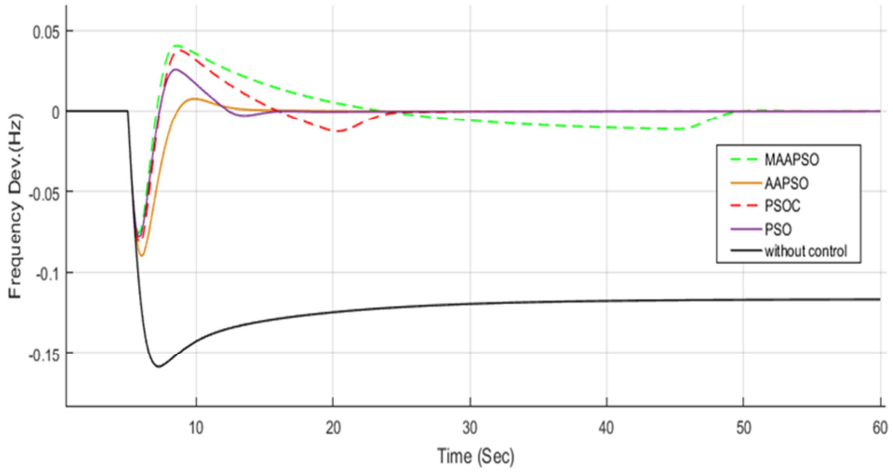

Figure 11. *Comparisons between 4 gains for Frequency Deviation in LLS in case of FO-PI controller.*

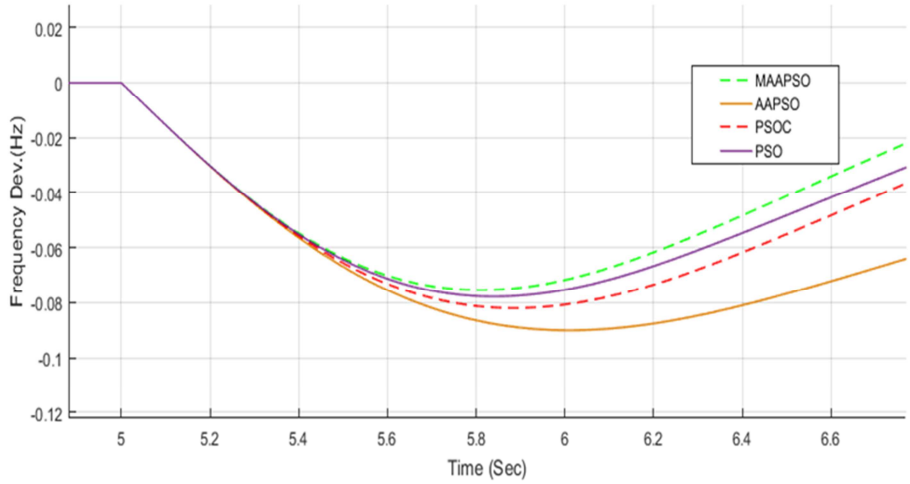

Figure 12. *Zoomed in System frequency response (ROCOF) in case of FO-PI controller.*

As illustrated in Figure 11; it is obvious that the error (frequency deviation) is inherent in the frequency system response due to the occurred disturbance load which mean that the system by itself without controller can't resolve the disturbance. Despite the AAPSO gain shows the lowest (best) values for both the maximum overshoot and settling time but it presents highest (worst) values for both the Nadir point and ROCOF compared with other gains while in contrast the MAAPSO appears the lowest (best) values for both Nadir point and ROCOF whilst offering the highest (worst) values for both maximum overshoot and settling time compared with other gains.

PSO gain indicates moderated and good performance gives 2nd lowest (best) values for all compared parameters like Nadir point, maximum overshoot, ROCOF compared with other gains while PSOC shows 3rd best values for same parameters.

The best objective function index were gained during the run of iterations for each type of PSO individually are: MAAPSO, AAPSO, PSOC, respectively while the highest Objective function index (which mean longer time to obtain acceptable solution) was gain PSO.

6. Conclusion

The suggested PSO-based FO-PI and PI controllers is studied for the three major issues of the SEPS:

a) System parameter variations as a result of changes in operating condition,

b) Non-linearity in the interactions.

These studies are completed firstly, by applying the Proportional Integral controller on two SEPS loading situations representing highest (Maximum) and lowest (Minimum) peak load of the SEPS separately and studding the effect of tripping of biggest unit in SEPS (K- 650 MW) then apply same two loading situations on Fraction Order –PI controller to compare the performance of both controller.

The model used in this paper was developed and built on the dynamic model of the National Energy Control Center (NECC) by updating Combined Cycle units in addition to Wind units models to original model of (NECC) which is formed in 1992 to contain the new conventional power stations statistics till 2019-2020. Then using various types of suggested PSO algorithms to acquire the controller gain to annihilate the frequency deviation (error) caused by the disturbance (outage load) occurred in both two loading situations, which could be generalized to any loading situation.

The application of the suggested FO-PI controllers based on PSO present enhancement in the dynamic frequency response performance of the SEPS according to ROCOF, Settling Time, Maximum Overshoot, Nadir and well damping in a wide range of operating conditions. Even in the existence of Generating Rate Constraints (GRC), which confirms its strength. The achieved results are promising in this field.

References

[1] Elgerd, O. I., and C. E. Fosha. 1970. "Optimum megawatt-frequency control of multiarea electric energy systems". IEEE transactions on power apparatus and systems 4: 556-563. doi: 10.1109/tpas.1970.292602.

[2] Tripathy, S. C., G. S. Hope, and O. P. Malik. 1982."Optimisation of load-frequency control parameters for power systems with reheat steam turbines and governor deadband nonlinearity". IEE Proceedings C Generation, Transmission and Distribution (129) 1: 10-16. doi: 10.1049/ip-c.1982.0002.

[3] Ebrahim, M. A., M. Becherif, and A. Y. Abdelaziz. 2021."PID-/FOPID-based frequency control of zero-carbon multisources-based interconnected power systems underderegulated scenarios". International Transactions on Electrical Energy Systems 31 (2). doi: 10.1002/2050-7038.12712.

[4] Ali, Ali M., M. Ebrahim, and M. A Moustafa Hassan. 2016." Automatic voltage generation control for two area power system based on particle swarm optimization". Indonesian Journal of Electrical Engineering and Computer Science 2 (1): 132-144. doi: 10.11591/ijeecs.v2.i1.pp132-144.

[5] Hussein, A. A., N. Hasan, I. Nasirudin, and S. Farooq. 2020. "Load frequency controller for multisource interconnected nonlinear power system incorporating FACTs devices". International Journal of Automation and Control 14 (3): 257-283. doi: /10.1504/IJAAC.2020.107082.

[6] Zhu, G., L. Nie, Z. Lv, L. Sun, X. Zhang, and C. Wang. 2020."Adaptive fuzzy dynamic surface sliding mode control of large-scale power systems with prescribe output tracking performance". ISA transactions 99: 305-321. doi: 10.1016/j.isatra.2019.08.063.

[7] Jagatheesan, K., and, B. Anand. 2018. "AGC of multi-area hydro-thermal power systems with GRC non-linearity and classical controller". Journal of Global Information Management (JGIM) 26 (3): 11-24. doi: 10.4018/JGIM.2018070102.

[8] EEHC (Egyptian Electricity Holding Company) 2018/2019 Annual Report. http://www.moee.gov.eg/test_new/report.aspx.

[9] Alhelou, H. H., Hamedani-Golshan, M. E., Zamani, R., Heydarian-Forushani, E., & Siano, P. (2018). Challenges and opportunities of load frequency control in conventional, modern and future smart power systems: a comprehensive review. Energies, 11 (10), 2497.

[10] Zurfi, A., & Zhang, J. (2016). Exploitation of battery energy storage in load frequency control-a literature survey. Am. J. Eng. Applied Sci, 9, 1173-1188.

[11] Obaid, Z. A., Cipcigan, L. M., Abrahim, L., & Muhssin, M. T. (2019). Frequency control of future power Systems: reviewing and evaluating challenges and new control methods. Journal of Modern Power Systems and Clean Energy, 7 (1), 9-25.

[12] Wu, Z.; Gao, W.; Gao, T.; Yan, W.; Zhang, H.; Yan, S.; Wang, X. State-of-the-art review on frequency Response of wind power plants in power systems. J. Mod. Power Syst. Clean Energy 2018, 6, 1–16.

[13] Bevrani, H.; Hiyama, T. Intelligent Automatic Generation Control, 1st ed.; CRC Press: Boca Raton, FL, USA, 2017.

[14] Shankar, R.; Pradhan, S.; Chatterjee, K.; Mandal, R. A comprehensive state of the art literature survey On LFC mechanism for power system. Renew. Sustain. Energy Rev. 2017, 76, 1185–1207.

[15] Pandey, S.; Mohanty, S.; Kishor, N. A literature survey on load frequency control for conventional and Distribution generation power systems. Renew. Sust. Energy. Rev. 2013, 25, 318–334.

[16] Yassin, K., E. Abd-Raboh, and M. S. Al-Domany. 1992."Fast Power System Restoration via Load Shedding Practices in Egyptian Power System". Mansoura Eng. Journal 17 (1): 1-20. doi: 10.21608/bfemu.2021.166762.

[17] Mai, M. A, M. H. Soliman, and H. A. Talaat. 2018."Integration Impact of Wind Energy Conversion Systems on the Egyptian Power System". Second International Conference New Trends in Sustainable Energy (ICNTSE), Pharos University, Egypt: 18-19.

[18] Mai, M. A, M. H. Soliman, and H. A. Talaat. 2019. "Particle Swarm-Based Load Frequency Control for Enhancing Wind Turbine Contribution". Engineering and Scientific Research Journal (ESRJ), Shoubra Faculty of Engineering, Benha University, Egypt 1 (40): 112-120.

[19] Aziz, A., A. T. Oo, and A. Stojcevski. 2018. "Analysis of Frequency Sensitive Wind Plant Penetration Effect on Load Frequency Control of Hybrid Power System". International Journal of Electrical Power & Energy Systems 99: 603-17. doi: 10.1016/j.ijepes.2018.01.045.

[20] Ali, Ali M., M. Ebrahim, and M. A Moustafa Hassan. 2015."Control of single area power system based on evolutionary computation techniques". IEEE 17th International Middle East Power Systems Conference (MEPCON'2015), Mansoura University, Egypt: 16: 19.

[21] Eiben, A. E., and J. E. Smith. 2015. Evolutionary computing: the origins: Introduction to Evolutionary Computing. Springer, Berlin, Heidelberg: 13-24. doi: 10.1007/978-3-662-44874-8_2.

[22] Ebrahim, M. A., Ali M. Ali, and M. A Moustafa Hassan. 2017a."Frequency and voltage control of multi area power system via novel particle swarm optimization techniques". International Journal of Computer Research 24 (4): 427-474.

[23] Singh, S. N., J. Ø Stergaard, and J. Yadagiri. 2009. "Application of advanced particle swarm optimization techniques to wind-thermal coordination".15th International Conference on Intelligent System Applications to Power Systems, IEEE: 1-6. doi: 10.1109/isap.2009.5352912.

[24] Balu, Korra, and Vivekananda Mukherjee. 2020." Siting and Sizing of Distributed Generation and Shunt Capacitor Banks in Radial Distribution System Using Constriction Factor Particle Swarm Optimization. Electric Power Components and Systems 48 (6-7): 697-710. doi: 10.1080/15325008.2020.1797935.

[25] Ebrahim, M. A., Ali M. Ali, and M. A Moustafa Hassan. 2017b." Frequency and Voltage Control of Multi Area Power System via Novel Particle Swarm Optimization Techniques". In "Particle Swarm Optimization (PSO)". edited by Walker, Brian: 39-97. Nova Science Publishers, Incorporated. ISBN: 978-1-53610-846-0.

[26] Ahmed, S., B. Tarek, and N. Djemai. 2013. "Economic dispatch resolution using adaptive acceleration coefficients based PSO considering generator constraints". International Conference on Control, Decision and Information Technologies (CoDIT), May: 212-217: doi: 10.1109/CoDIT.2013.6689546.

[27] Abbas, Ghulam, Jason Gu, Umar Farooq, Muhammad Usman Asad, and Mohamed El-Hawary. 2017." Solution of an economic dispatch problem through particle swarm optimization: a detailed survey-part I". IEEE Access 5: 15105-15141. doi: 10.1109/access.2017.2768522.

[28] Khalifa, F., M. Moustafa Hassan, Osama Abul-Haggag, and Hassan Mahmoud. 2015."The application of evolutionary computational techniques in medium term forecasting". Presentation at MEPCON.

[29] Hägglund, Tore, and K. J. Åström. 2000."Supervision of adaptive control algorithms." Automatica 36 (8): 1171-1180.

[30] Konak, A., D. W. Coit, and A. E. Smith. 2006. "Multi-objective optimization using genetic algorithms: A tutorial". Reliability engineering & system safety 91 (9): 992-1007. doi: 10.1016/j.ress.2005.11.018.

[31] Ali, A. M., Saad, M. A. S., El-Amari, A. A., & Hassan, M. A. M. 2021. Automatic Generation Control of an Interconnected Power System. International Journal of Ambient Energy, 1-21., doi: 10.1080/01430750.2021.1969273.